Eur. Phys. J. A **27**, 257–262 (2006)
DOI 10.1140/epja/i2005-10273-1

THE EUROPEAN PHYSICAL JOURNAL A

Letter

New information on the $T_{1/2} = 47$ s isomer in the ^{136}I nucleus

W. Urban[1,a], M. Saha Sarkar[2], S. Sarkar[3], T. Rząca-Urban[1], J.L. Durell[4], A.G. Smith[4], J.A. Genevey[5], J.A. Pinston[5], G.S. Simpson[6], and I. Ahmad[7]

[1] Faculty of Physics, Warsaw University, ul.Hoża 69, 00-681 Warsaw, Poland
[2] Saha Institute of Nuclear Physics, 1/AF Bidhan Nagar, Kolkata 700064, India
[3] Department of Physics, The University of Burdwan, Golapbag, Burdwan 713104, India
[4] Department of Physics and Astronomy, University of Manchester, Manchester M13 9PL, UK
[5] Laboratoire de Physique Subatomique et de Cosmologie, IN2P3-CNRS/Université J. Fourier, F-38026 Grenoble Cedex, France
[6] Institut Laue-Langevin, 6 rue Jules Horowitz, F-38042 Grenoble Cedex 9, France
[7] Argonne National Laboratory, Argonne, IL 60439, USA

Received: 12 September 2005 / Revised version: 17 March 2006 /
Published online: 4 May 2006 –
Communicated by D. Schwalm

Abstract. The ^{136}I nucleus, populated in the spontaneous fission of ^{248}Cm, was studied by means of prompt γ-ray spectroscopy using the EUROGAM2 array. The observation in this work of the 42.6 keV prompt-γ, $M1 + E2$ transition de-exciting the 7^- level in ^{136}I indicates that this level, interpreted as the $(\pi g_{7/2}^3 \nu f_{7/2})_{7^-}$ configuration, does not correspond to the $T = 47$ s, β-decaying isomer in ^{136}I. The isomer is placed 42.6 keV below the 7^- level. It has spin 6^- and is interpreted as the $(\pi g_{7/2}^2 d_{5/2} \nu f_{7/2})_{6^-}$ configuration. This and other members of both multiplets can be reproduced properly only if one assumes that the $\pi d_{5/2}$ orbital in ^{136}I is located 400 keV lower than in ^{133}Sb. Possible mechanisms causing this effect are discussed.

PACS. 21.10.-k Properties of nuclei; nuclear energy levels – 21.10.Tg Lifetimes – 25.85.Ca Spontaneous fission – 27.60.+j $90 \leq A \leq 149$

It is expected that at the surface of nuclei with large neutron excess the distribution of neutrons will be diffused, which may significantly influence energies of single-particle orbitals [1–4]. One possible reason is the decrease of the spin-orbit strength in neutron-rich nuclei [2,3]. Another cause can be simulated by the decrease of the l^2 term in the Nilsson potential [5]. Both effects lead to the diminishing of the shell structure in very neutron-rich nuclei. The experimental verification of these predictions is of prime importance for the understanding of nuclear interactions, in general, and for the studies of the astrophysical r-process, in particular [6].

Recent measurements by Schiffer *et al.* [7] of the energy splitting between the $1i_{13/2}$ and $1h_{9/2}$ neutron orbitals above the $N = 82$ shell and the $1h_{11/2}$ and $1g_{7/2}$ proton orbitals above the $Z = 50$ shell suggest that at $N - Z = 32$ the spin-orbit interaction may decrease to half of its maximum value observed around the stability line ($N - Z \approx 20$). It is important to note that this effect grows *gradually* with the $N - Z$ value, as illustrated in fig. 1, drawn after ref. [7] to help further discussions.

In the ^{135}Sb nucleus the first excited $5/2^+$ level was found at an energy of 282 keV [10,8]. The $d_{5/2}$ proton excitation in ^{133}Sb is located at 962 keV. In both nuclei the ground state is interpreted as the $g_{7/2}$ proton orbital. In fig. 1b we show (after ref. [8]) the energy difference, $\Delta E3$, between the $2d_{5/2}$ and $1g_{7/2}$ proton orbitals. It grows smoothly up to $N - Z = 31$, where a sudden drop occurs in ^{135}Sb (black dot). This surprising effect was discussed in refs. [8,11] as due to the decrease of the l^2 term predicted in refs. [4,5] to occur at the diffused nuclear surface of neutron-rich nuclei. Reference [11] presents also calculations of proton single-particle energies which, according to the authors, supports the presence of the so-called neutron skin. In this picture the neutron skin appears quite suddenly above $N = 82$ and, what is also surprising, the effect weakens above $N = 90$ (see fig. 16 in ref. [11]).

It is interesting to ask if this puzzling decrease in the position of the $d_{5/2}$ proton level can be seen in other nu-

[a] e-mail: urban@fuw.edu.pl

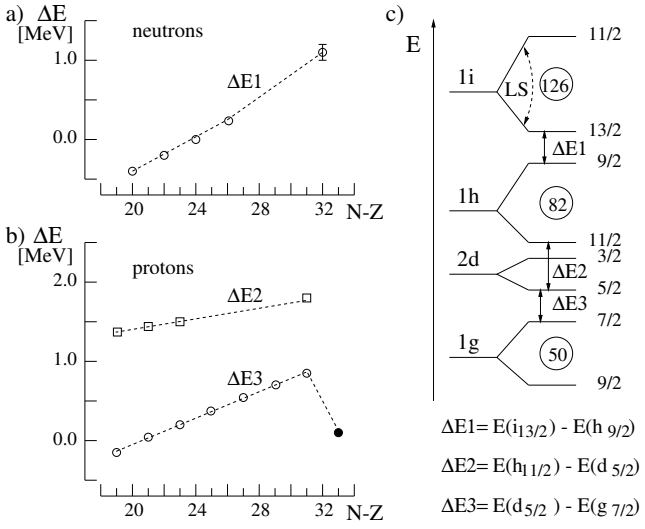

Fig. 1. Energy differences, ΔE, between various a) neutron and b) proton orbitals above $N = 82$ and $Z = 50$, respectively, as schematically defined in part c). The data are taken from refs. [7,8] and [9] (for ^{134}Sb). See the text for more explanations.

clei from the region. No data is available on higher-mass Sb isotopes at present but the shell model $d_{5/2}$ proton excitation can be traced in neutron-rich iodine isotopes.

The ^{136}I nucleus was studied before [12] in a measurement of prompt γ-rays following the spontaneous fission of ^{248}Cm, using EUROGAM2 array. The medium-spin part of its excitation scheme starts with the 1111.3 keV, $E2$ transition populating the $I^\pi = 7^-$ member of the $(\pi g_{7/2}^3 \nu f_{7/2})_j$ multiplet. No decay out of this level was observed in ref. [12], which might suggest its isomeric character. The conventional shell model calculations, using the 962 keV energy of the $\pi d_{5/2}$ level predict the $(\pi g_{7/2}^3 \nu f_{7/2})_{7^-}$ configuration for the isomer. On the other hand, the 47 s isomer in ^{136}I was reported with spin and parity $I^\pi = 6^-$ [13]. Therefore, ref. [12] proposed that the isomer with spin 6^- is located just below the $(\pi g_{7/2}^3 \nu f_{7/2})_{7^-}$ level and is not observed because of a small distance between the two levels (estimated in ref. [12] as less than 60 keV). In this context it is worth mentioning a recent study of low-spin excitations in ^{136}I [14], in which the $(\pi g_{7/2}^3 \nu f_{7/2})_{7^-}$ configuration is assigned to the 47 s isomer. We also note here that the excitation energy of the 47 s isomer, reported at about 640 keV [13,15,16], is far off any conventional shell model predictions.

The study reported in ref. [12] was made at an early stage of the analysis of the data from our EUROGAM2 measurement. Later improvements to the analysis techniques [9] enabled studies at higher sensitivity level as well as at lower γ-ray energies, measured by Low-Energy-Photon (LEP) spectrometers attached to the EUROGAM [17]. With these improvements we reinvestigated neutron-rich iodine isotopes. Full account of these studies will be given in a forthcoming article while in this letter we report on some important observations, concerning the 47 second isomer in ^{136}I.

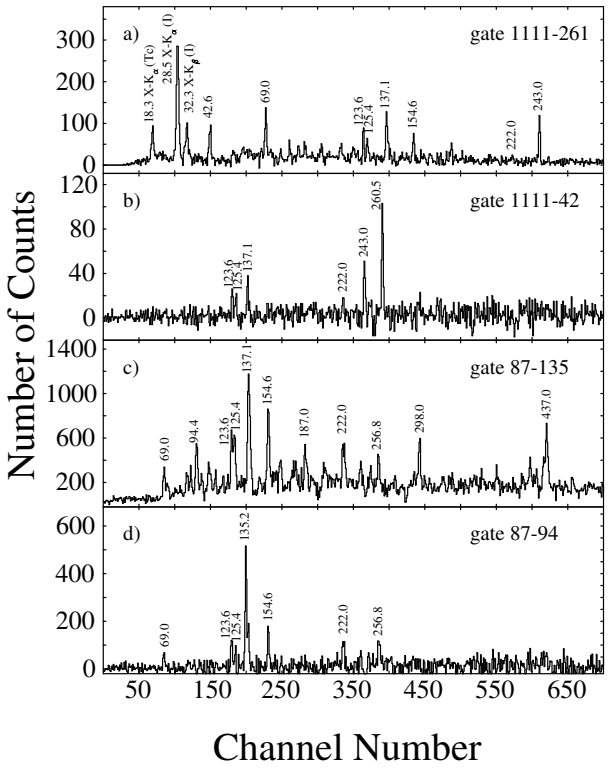

Fig. 2. Coincidence spectra of γ-rays following the fission of ^{248}Cm, gated on lines in ^{136}I. Lines are labeled with their energies in keV. Spectrum a) is measured by LEP while the other spectra are measured by the Ge detector of EUROGAM. See the text for more explanations.

In the LEP spectrum, double gated on the 260.6 keV and 1111.3 keV lines of ^{136}I, which is shown in fig. 2a, one can see the 243.0 keV line of ^{136}I, the 69.0 keV, 123.6 keV, 125.4 keV, 137.5, 154.6 keV and 222.0 keV known lines from the complementary ^{108}Tc, ^{109}Tc and ^{110}Tc isotopes as well as the technetium K_α, X-ray line at 18.3 keV. The dominating line in the spectrum is the iodine K_α, X-ray line at 28.5 keV. We note that such high intensity of the iodine K_α line cannot be due to the conversion of the 243.0 keV line of ^{136}I. In the spectrum there is a new line at 42.6 keV. The spectrum doubly gated on the 1111.3 keV and 42.6 keV lines displayed in fig. 2b contains again lines of ^{136}I, ^{108}Tc, ^{109}Tc and ^{110}Tc, indicating that the 42.6 keV line belongs to ^{136}I. The coincidences seen in figs. 2a and b and further gates show that the 42.6 keV transition is located in the decay scheme below the 1111.3 keV transition.

From fig. 2a we deduced the α_K conversion coefficient for the 42.6 keV transition, taking the observed intensities of the 28.5 keV, 42.6 keV and 243.0 keV lines and assuming a maximum conversion coefficient of 0.08 for the 243.0 keV, $M1 + E2$ transition. The resulting value of $\alpha_K = 7(1)$ indicates the $\Delta I \leq 1$, $M1 + E2$ character of the 42.6 keV transition. This is consistent with spin and parity $I^\pi = 6^-$ for the level populated by the 42.6 keV transition, which could, thus, correspond to the 47 s, 6^- isomer proposed in [13]. The upper limit for the intensity

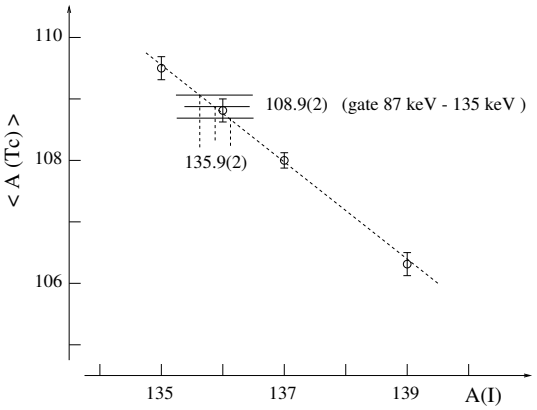

Fig. 3. Mass correlation diagram for Tc and I isotopes and the identification of the low-spin gamma cascade in ^{136}I. See text for more explanations.

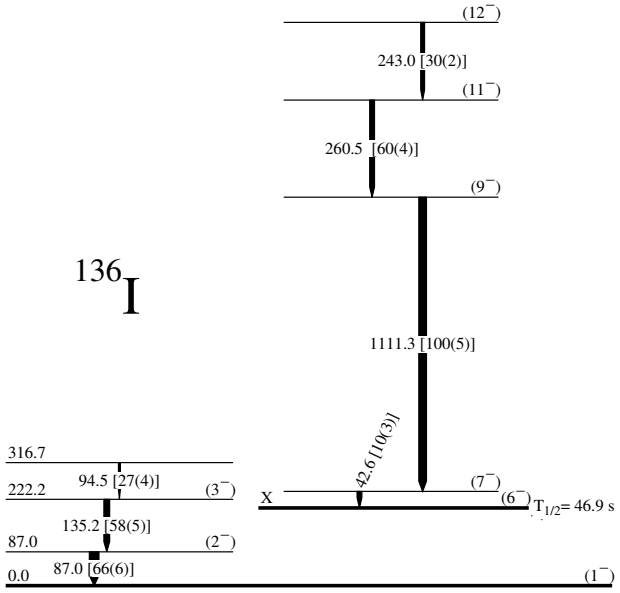

Fig. 4. Partial scheme of low-energy excitations in ^{136}I as obtained in the present work. Transition and excitation energies are given in keV. In square brackets are relative prompt-gamma intensities as observed in the spontaneous fission of ^{248}Cm.

of the (unobserved) $(1111 + 43)$ keV cross-over transition from the 9^- level is 1.2×10^{-3}. This is consistent with the proposed spin 6 of the isomer.

In the low-spin part of the ^{136}I excitation scheme a cascade of 87.3 keV and 135.4 keV transitions was reported [15,18,19]. We note an inconsistency between these energies and the energy of the first excited state at 86.7 keV. In this work we observe transitions at 87.0 keV and 135.2 keV. The spectrum double gated on these transitions, shown in fig. 2c, contains lines belonging to the $^{108-110}$Tc nuclei. These cross-coincidences indicate the prompt-gamma character of the 87.0 keV and 135.2 keV lines populated in the fission of ^{248}Cm. In fig. 2c one also sees a new line at 94.5 keV. The 87 keV-94 keV double gate, displayed in fig. 2d, shows the 135.2 keV line and lines of $^{108-110}$Tc nuclei indicating that the 94.5 keV transition is in cascade with the 87.0 keV and 135.2 keV transitions in ^{136}I.

The assignment of the 87.0 keV and 135.2 keV lines to ^{136}I is confirmed by the mass correlation technique [20] presented in fig. 3. The application of this technique to the I-Tc pairs of fission fragments is described in more detail in refs. [21,22], from where we took experimental points for ^{135}I, ^{137}I and ^{139}I. The point for ^{136}I is obtained from a spectrum gated on the 1111.3 keV and 260.6 keV lines of ^{136}I. The horizontal bars in fig. 3 represent the average Tc mass with its error, $\langle \mathrm{Tc} \rangle = 108.9(2)$, calculated from intensities of lines in ^{108}Tc, ^{109}Tc and ^{110}Tc observed in the spectrum gated on the 87 keV-135 keV cascade (fig. 2c). The intersection of these bars with the straight-line fit to the data points (dashed line in fig. 3), uniquely correlates the 87.0 keV-135.2 keV cascade with the ^{136}I nucleus.

We could determine the α_K conversion coefficient for the 87.0 keV transitions from its gamma intensity compared with the intensity of the iodine K_α, X-ray line at 28.5 keV line in a spectrum doubly gated on the 135.2 keV line from ^{136}I and the 69.0 keV line from ^{109}Tc. The resulting value, $\alpha_K = 3.2(8)$, indicate the $M1 + E2$ character of this transition, confirming previous works [15].

The above results have important consequences for spin assignments in the low-spin part of the ^{136}I level scheme. It is commonly observed that fission process populates predominantly those states in fission-fragment nuclei, which are close to the yrast line. Consequently, spins increase with the excitation energy in γ-ray cascades populated in fission. Therefore, assuming spin $I = 1$ for the ground state in ^{136}I after the literature [15], we propose spins $I = 2$ for the 87.0 keV level and $I = 3$ for the 222.2 keV level, instead of previously assigned values [15]. The new, tentative level at 316.7 keV should have spin higher than 3, according the "yrast population" argument. We assume here that the 94.5 keV transition corresponds to $\Delta I = 1$ because a stretched $E2$ transition of this energy in ^{136}I would require a half-life of the order of 100 ns for the 317 keV level, which is not observed. Thus, we tentatively assign spin 4^- to the 317 keV level. The partial scheme of low-energy excitations in ^{136}I, as observed in this work, is shown in fig. 4.

The newly placed 6^- level, is shown in fig. 4 below the 222.2 keV, 3^- level because the difference between the spin of the isomer and the spin of the first level below the isomer should be larger than three, considering the 47 s half-life and *zero* gamma decay branch of the isomer [15]. A very low energy, the unobserved $M3$, cannot be fully rejected, however, which would correspond to the position of the isomer just above the 222.2 keV, 3^- level. In either case, the isomer is located at about 0.2 MeV above the ground state, in contrast to the 0.6 MeV reported in the literature [15,16]. This low energy of the isomer, which is similar to the low energy of the analogous 7^- isomer within the $(\pi g_{7/2} \nu f_{7/2})_j$ multiplet in ^{134}Sb [23], is supported by shell model calculations with the KH5082 set

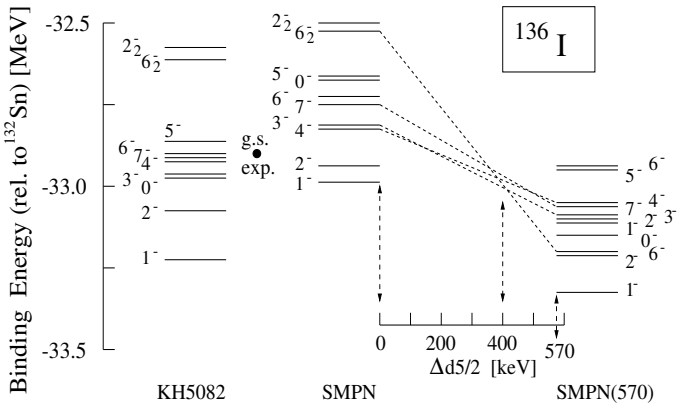

Fig. 5. Comparison of calculated (relative to the ground state of ^{132}Sn) binding energies for low-spin levels in ^{136}I. The data are from this work and refs. [16,15]. See the text for explanations.

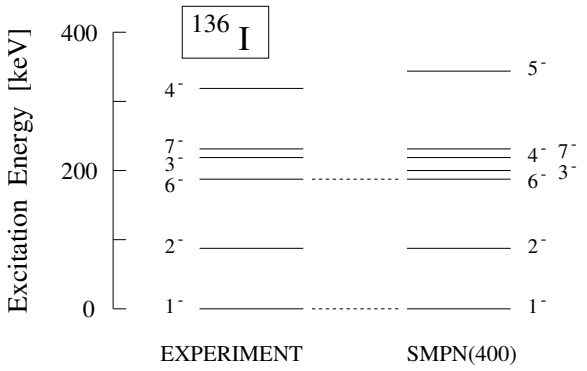

Fig. 6. Comparison of calculated and experimental excitation energies within the $(\pi g_{7/2}\nu f_{7/2})$ and $(\pi d_{5/2}\nu f_{7/2})$ multiplets in the ^{136}I nucleus. The 1^- and 6^- levels are drawn at the same excitation energy, respectively. See the text for more explanations.

of two-body matrix elements (tbme), but also with an improved set, SMPN [24], as shown in fig. 5. The SMPN interactions describe better the experimental binding energy of the ground state, shown as a filled circle in fig. 5, but, similarly to KH5082 interactions, predict that the isomeric state has spin 7^-.

The SMPN interactions were tested on the ^{135}Sb nucleus where it was found that the first excited $5/2^+$ state can be reproduced only if the position of the $\pi d_{5/2}$ orbital is lowered by 570 keV. This confirms the unusual behavior of the $\pi d_{5/2}$ orbital reported in [11]. When applied to ^{136}I, the SMPN interactions with the $\pi d_{5/2}$ orbital lowered by 570 keV, (SMPN(570)), provide results as shown in fig. 5. All levels are lowered compared to SMPN (since one of the s.p. energies is decreased) but interestingly, the second 6^- level of the SMPN scheme decreases faster than the 7^- level.

It appears that the wave function of the 7^- state contains the odd proton in the $g_{7/2}$ orbital while the 6_2^- state, which becomes 6_1^- in the SMPN(570) scheme, is dominated by the $\pi g_{7/2}^2 d_{5/2}\nu f_{7/2}$ and $\pi d_{5/2}^3\nu f_{7/2}$ configurations, explaining its rapid decrease.

The SMPN(570) interactions provide the required 6^- spin for the isomer but the distance form 7^- to 6^- is too large. However, a simple, linear interpolation, sketched in fig. 5 helps to find the solution. Following the interpolated positions of levels as a function of the decrease of the $\pi d_{5/2}$ orbital, $\Delta d_{5/2}$, one finds that at $\Delta d_{5/2} = 400$ keV the 7^- to 6^- distance is close to that observed experimentally. Moreover, at this point the 6^- drops below the 4^- and 3^- levels to form a long-lived isomer. The partial half-life for the electromagnetic decay is calculated at 10^6 seconds, nicely explaining the non-observation in the experiment of any gamma decay branch for the 47 s isomer in ^{136}I. Excitation energies calculated with the SMPN interactions and the $\pi d_{5/2}$ orbital lowered by 400 keV, (SMPN(400)), are compared in fig. 6 with experimental data. The 6^- level, for which the experimental excitation energy is not known, is plotted at 187 keV, the calculated position of the 6^- level. The experimental excitations are taken from fig. 4. The reproduction of the 2^- and 3^- levels is very good, as well as the reproduction of the distance between the 6^- and 7^- levels (calculated at 45 keV). The 4^- level is calculated 103 keV below the experimental 4^- candidate at 317 keV. We note that the 317 keV level is closer to the theoretical 5^- level calculated at 346 keV.

This work have shown again the unusual property of the $\pi d_{5/2}$ orbital in the ^{132}Sn region, that it has to be significantly lowered, compared to its position in ^{133}Sb, in order to reproduce the properties of ^{135}Sb and ^{136}I nuclei. While further confirmation of this effect in other nuclei of the region will be valuable, one sees already now, that there is a new effect in the ^{132}Sn region, awaiting an explanation.

The proposition of ref. [8] that this is due to an appearance of a neutron skin above the $N = 82$ shell is now even less likely since the ^{136}I nucleus has only one neutron more than ^{133}Sb. Consequently, the formation of the neutron skin should be then very rapid, while there are arguments that it happens gradually. As seen in fig. 1, the split between various neutron and proton orbitals grows gradually with $N - Z$. Reference [7] proposed that this smooth increase results from the influence of the neutron excess on the single-particle energies. The data from fig. 1 can be described quantitatively to support this idea.

The spin-orbit interaction, $\boldsymbol{ls}$, acting on an orbital with the total momentum $j = l + s$, where l is the orbital angular momentum and s is the spin of a nucleon reads $V_{ls} = -B(r)\boldsymbol{ls}$. An important factor in the $B(r)$-function (the Thomas term) is the $\frac{\mathrm{d}V(r)}{\mathrm{d}r}$ derivative, where $V(r)$ is a nuclear potential and r is the distance from the center of a nucleus. In a realistic potential (*e.g.*, a Woods-Saxon type) this term has a maximum at the surface of a nucleus. Therefore the $B(r)$ will strongly depend on any changes to the surface diffuseness. After ref. [7] we assume that the energy differences shown in fig. 1 are due to changes in the $\boldsymbol{ls}$ interaction, caused by the increase in the diffuseness of the nuclear surface when the neutron excess, $N-Z$, grows.

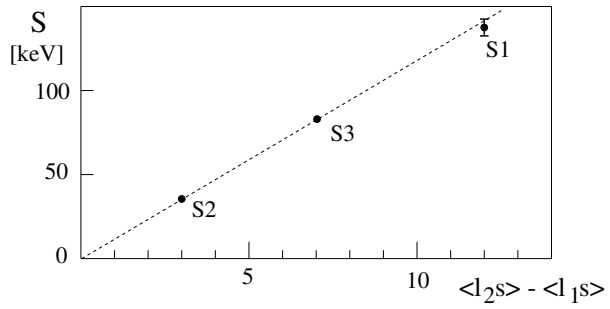

Fig. 7. Slopes of the ΔE curves from fig. 1 as a function of $\langle l_2 s\rangle - \langle l_1 s\rangle$. See the text for further explanations.

For the orbital with spin j the energy shift due to the $\boldsymbol{ls}$ interaction, is proportional to $-B(r)\langle ls\rangle$. Then, the energy difference between two orbitals with spins j_1 and j_2 is $\Delta E(j_1, j_2) = \Delta E_0 + B(r)(\langle l_2 s\rangle - \langle l_1 s\rangle)$, where ΔE_0 is the energy difference at zero spin-orbit interaction. Figure 1 shows that the ΔE value is proportional to $N-Z$, suggesting that $B(r) = C(N-Z)$, where C is a constant. Then the average slope of the ΔE-curve over the $N-Z$ range, $S = \frac{\Delta(\Delta E)}{\Delta(N-Z)}$, reads $S = C(\langle l_2 s\rangle - \langle l_1 s\rangle)$ and depends on the $\boldsymbol{ls}$ interaction, only.

We can check how well this picture fits the experiment. The expected value of the $\boldsymbol{ls}$ operator is $\langle ls\rangle = -(l+1)$ for $j = l - 1/2$ and $\langle ls\rangle = l$ for $j = l + 1/2$. Hence, the $\langle ls\rangle$ values are $+6$ for the $1i_{13/2}$ level, -6 for the $1h_{9/2}$ level, $+5$ for the $1h_{11/2}$ level, $+2$ for the $2d_{5/2}$ level and -5 for the $1g_{7/2}$ level. From this we calculate the $(\langle l_2 s\rangle - \langle l_1 s\rangle)$ value of 12 for $\Delta E1$, 3 for $\Delta E2$ and 7 for $\Delta E3$ curves from fig. 1. We take $\Delta(N-Z)$ ranges from 19 to 31 for protons and from 22 to 32 for neutrons (the latter is limited to avoid the data near the stability line, where the ΔE slopes change sign —see ref. [7]). Over such $\Delta(N-Z)$ ranges the ΔE changes by 1360(50) keV, 1000(1) keV and 403(1) keV for the $\Delta E1$, $\Delta E2$ and $\Delta E3$, respectively. The corresponding slopes are then $S1 = 136(5)$ keV, $S2 = 34$ keV and $S3 = 83$ keV per $N-Z$ unit. The uncertainties of the $S2$ and $S3$ are negligible. The error of the $S1$ originates from large uncertainty on the position of the $1i_{13/2}$ orbital [9,23].

The calculated slopes are plotted in fig. 7 against the corresponding $\langle l_2 s\rangle - \langle l_1 s\rangle$ values. One observes a striking correlation for the two proton slopes, $S2$ and $S4$, which fit very precisely a straight line crossing the (0,0) point. The ratio $S/(\langle l_2 s\rangle - \langle l_1 s\rangle)$, calculated for the $S1$, $S2$ and $S3$, varies by less than 3% around the average. The $S1$ point fits the line surprisingly well, considering that the effect for neutrons is obtained from a different chain of nuclei than that used to obtain the proton effect. The observed correlation supports the proposition of ref. [7] that the effects connected with neutron excess in nuclei increase gradually with this excess, starting already at the stability line. Therefore, the rapid decrease of the $d_{5/2}$ proton orbital above $N = 82$ seems to be a local effect, caused by a mechanism other than the surface diffuseness.

There are other puzzling observations in the ^{132}Sn region: i) in the KH5082 set of tbme's constructed for the ^{132}Sn region [25] from the interactions for the ^{208}Pb region by scaling according to the nuclear mass, some of the tbme's were in addition multiplied by an *ad hoc* factor, 0.6, to fit the experiment (see ref. [26] for details); ii) the $\pi d_{5/2}$ orbital has to be lowered in ^{136}I, but the low-spin excitations in its isotone ^{134}Sb are well reproduced by conventional shell model calculations [23]. Also the position of the $i_{13/2}$ level, deduced from the medium-spin excitations in ^{134}Sb, using conventional shell model estimates [9] fits the regular trend in figs. 1 and 7; iii) in ^{136}Te, which has four nucleons outside the ^{132}Sn core, the characteristic $(\pi g^2_{7/2}\nu f^2_{7/2})_{12^+}$ level [27,28] could be reproduced only after modifications of several tbme's [24]. Its position was also predicted correctly by the relativistic mean-field calculations, but with a modified spin-orbit interaction [2]; iv) it was found that shell model calculations give too high binding energies for ground states in the ^{132}Sn region [24, 26] (see also fig. 5). This overbinding shows some systematic properties as a function of the increasing N/Z ratio [24], suggesting either further modifications of tbme's or some of the s.p. energies, *e.g.*, $\nu f_{7/2}$. The above examples and the new unexplained effects found in this work indicate that a detailed theoretical investigations are in order to provide a proper description of the ^{132}Sn region.

In summary, we propose that the 47 s isomeric level in the ^{136}I nucleus has spin 6^- and corresponds to the $\pi g^2_{7/2} d_{5/2} \nu f_{7/2}$ configuration. To reproduce this level, the position of the $d_{5/2}$ orbital has to be lowered by 400 keV, compared to that in ^{133}Sb, which supports a similar observation in ^{135}Sb. We also provided arguments suggesting that structural changes due to the neutron excess appear gradually as a function of this excess. Thus the change in the position of the $d_{5/2}$ orbital may be due to a new, local effect in the region of the ^{132}Sn core, calling for an explanation.

The work was partly supported by the US Department of Energy under contract No. W-31-109-ENG-38. The authors are indebted for the use of ^{248}Cm to the Office of Basic Energy Sciences, US Department of Energy, through the transplutonium element production facilities at the Oak Ridge National Laboratory.

References

1. J. Dobaczewski *et al.*, Phys. Rev. Lett. **72**, 981 (1996).
2. X.Q. Zhang *et al.*, Phys. Rev. C **58**, R2663 (1998).
3. G.A. Lalazissis *et al.*, Phys. Lett. B **418**, 7 (1998).
4. I. Hamamoto *et al.*, Nucl. Phys. A **683**, 255 (2001).
5. B. Pfeiffer *et al.*, Acta Phys. Pol. B **27**, 475 (1996).
6. F.-K. Thieleman, K.-L. Kratz, *Proceedings of the XXII Masurian Lakes Summer School, Poland 1991* (IOP Publishing, Bristol, UK, 1992) pp. 187-226.
7. J.P. Schiffer *et al.*, Phys. Rev. Lett **92**, 162501 (2004).
8. J. Shergur *et al.*, Nucl. Phys. A **682**, 493c (2001).
9. W. Urban *et al.*, Eur. Phys. J. A **5**, 239 (1999).
10. A. Korgul *et al.*, Phys. Rev. C **64**, 021302(R) (2001).
11. J. Shergur *et al.*, Phys. Rev. C **65**, 034313 (2002).

12. P. Bhattacharyya *et al.*, Phys. Rev. C **56**, R2363 (1997).
13. W.R. Western *et al.*, Phys. Rev. C **15**, 1822 (1977).
14. A.J. Ass *et al.*, *NFL Studsvik*, Experimental Report (2002) p. 154.
15. *Evaluated Nuclear Structure Data File* (2005), `www.nndc.bnl.gov`.
16. G. Audi, A.H. Wapstra, C. Thibault, Nucl. Phys. A **729**, 337 (2003).
17. W. Urban *et al.*, Z. Phys. A **358**, 145 (1997).
18. F. Schussler *et al.*, Z. Phys. A **283**, 43 (1977).
19. U. Keyser *et al.*, Z. Phys. A **289**, 407 (1979).
20. M.C.A. Hotchkis *et al.*, Nucl. Phys. A **530**, 111 (1991).
21. W. Urban *et al.*, Phys. Rev. C **61**, 041301(R) (2000).
22. W. Urban *et al.*, Phys. Rev. C **62**, 044315 (2000).
23. A. Korgul *et al.*, Eur. Phys. J. A **15**, 181 (2002).
24. S. Sarkar, M. Saha Sarkar, Eur. Phys. J. A **21**, 61 (2004).
25. W.T. Chou, E.K. Warburton, Phys. Rev. C **45**, 1720 (1992).
26. S. Sarkar, M. Saha Sarkar, Phys. Rev. C **64**, 014312 (2001).
27. A. Nowak *et al.*, Eur. Phys. J. A **3**, 111 (1998).
28. A. Korgul *et al.*, Eur. Phys. J. A **7**, 167 (2000).